

Supporting Information

Rational Design and Optimization of a Potent IDO1 Proteolysis Targeting Chimera (PROTAC)

Authors: Paige J. Monsen,¹ Prashant V. Bommi,² Arabela A. Grigorescu,³ Kristen L. Lauing², Yingyu Mao,⁴ Payton Berardi,² Lijie Zhai², Oluwatomilayo Ojo,² Manon Penco-Campillo,² Taylor Koch,² Michael Egozi,² Sonam Jha,¹ Sara F. Dunne,⁴ Hong Jiang,⁵ Guiqin Song,⁵ Fang Zhang,⁵ Steven Kregel,^{2,6} Ali Vaziri-Gohar,^{2,6,7} Sean W. Fanning,² Pilar Sanchez-Gomez,⁸ Jacob M. Allen,⁹ Bakhtiar Yamini,¹⁰ Rimas V. Lukas,¹¹ Derek A. Wainwright,^{2,6,12*} Gary E. Schiltz^{1,13,14,*}

Affiliations: ¹Department of Chemistry, Northwestern University, Evanston, IL, USA. ²Department of Cancer Biology, Loyola University Chicago Stritch School of Medicine, Maywood, IL, USA. ³Department of Molecular Biosciences, Northwestern University Weinberg College of Arts and Sciences, Evanston, IL, USA. ⁴High-Throughput Analysis Laboratory, Chemistry of Life Processes Institute, Northwestern University, Evanston, IL, USA. ⁵HD Biosciences (China) Co. Ltd, a WuXi AppTec company, Shanghai 201201, China. ⁶Cardinal Bernardin Cancer Center, Maywood, IL, USA. ⁷Department of Surgery, Loyola University Chicago Stritch School of Medicine, Maywood, IL, USA. ⁸Neuro-oncology Unit, Unidad Funcional de Investigación en Enfermedades Crónicas (UFIEC), Instituto de Salud Carlos III (ISCIII), Madrid, Spain. ⁹Department of Health and Kinesiology, University of Illinois at Urbana-Champaign, Urbana, IL, USA. ¹⁰Department of Neurological Surgery, University of Chicago Medicine, Chicago, IL, USA. ¹¹Department of Neurology, Northwestern University Feinberg

School of Medicine, Chicago, IL, USA. ¹²Department of Neurological Surgery, Loyola University Medical Center, Maywood, IL, USA. ¹³Robert H. Lurie Comprehensive Cancer Center, Chicago, IL, USA. ¹⁴Department of Pharmacology, Northwestern University, Feinberg School of Medicine, Chicago, IL, USA.

Corresponding Authors:

*Gary E. Schiltz, Ph.D., Department of Chemistry, Pharmacology, and the Robert H. Lurie Comprehensive Cancer Center, Northwestern University. Phone: (847) 467-2287, Email: gary-schiltz@northwestern.edu.

*Derek A. Wainwright, Ph.D., Departments of Cancer Biology and Neurological Surgery, Laboratory of Brain Aging, Cancer Immunology, and Immunotherapy 2160 S. First Avenue, Bldg. 112., Maywood, IL 60153, Cardinal Bernardin Cancer Center, Room 202 Office #: (708) 327-3130; Lab #: (708) 327-2177, Loyola University Chicago Stritch School of Medicine, Email: dwainwr@luc.edu

Paige J. Monsen and Prashant V. Bommi contributed equally to this work.

Table of Contents

Figure S1. Kynurenine inhibition by active PROTAC 21 , inactive control 24 , and enzymatic inhibitor 4 (BMS-986205) in U87 and GBM43 cells.....	S4
Figure S2. Kynurenine inhibition by active PROTAC 21 , inactive control 24 , and enzymatic inhibitor 4 (BMS-986205) across multiple cell lines.....	S5
Figure S3. BLI data for Inactive IDO1 PROTAC 24 (NU227428).....	S6
Figure S4. Pharmacokinetics of 20 (NU227327).....	S7
¹ H-NMR, ¹³ C-NMR, and HPLC of key IDO1 Degraders.....	S8-S27
Figure S5. Raw western blot images used in Figure 5.....	S28
Figure S6. Raw western blot images used in Figure 6.....	S29

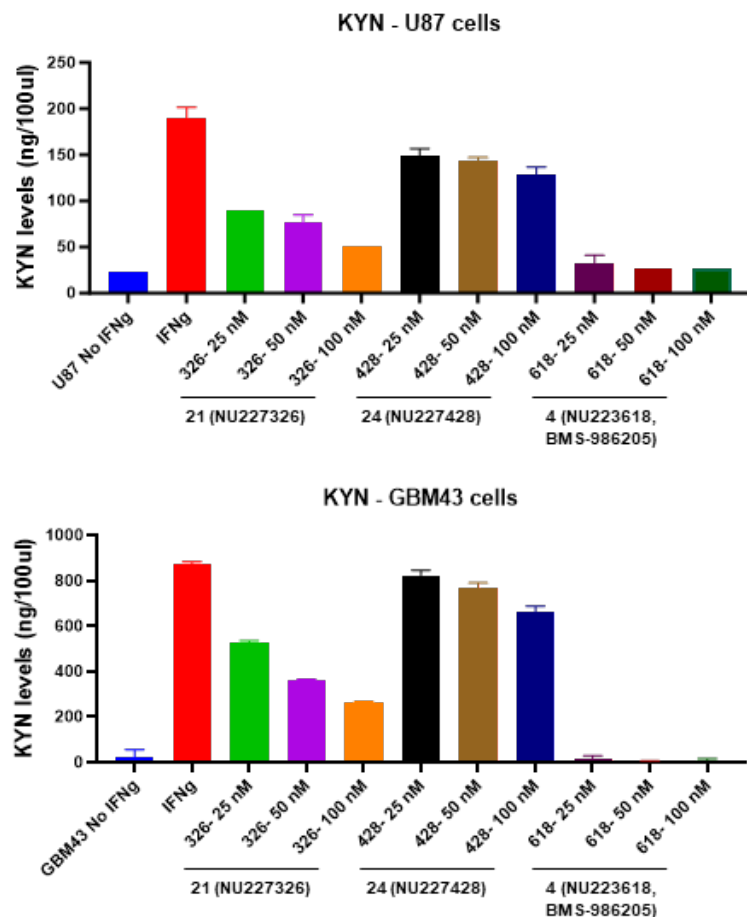


Figure S1. Inhibition of IDO1 enzyme activity by **21** (NU227326), inactive control compound **24** (NU227428), and **4** (NU223618, BMS-986205) in GBM cells. Supernatants from U87 and GBM43 cells were collected after 24-hour treatment with either compound **21** (NU227326), inactive PROTAC **24** (NU227428), or IDO1 enzyme inhibitor **4** (NU223618, BMS-986205) at indicated concentrations. Kynurenine levels in the supernatants were measured using a modified Ehrlich method. Where indicated, U87 cells were treated with 50 ng/mL IFN γ and GBM43 cells were treated with 10 ng/mL IFN γ . Data are presented as mean \pm SEM. Statistical significance was determined using Tukey's multiple comparison test for comparisons between more than two groups and an unpaired Student's t-test for comparisons between two groups.

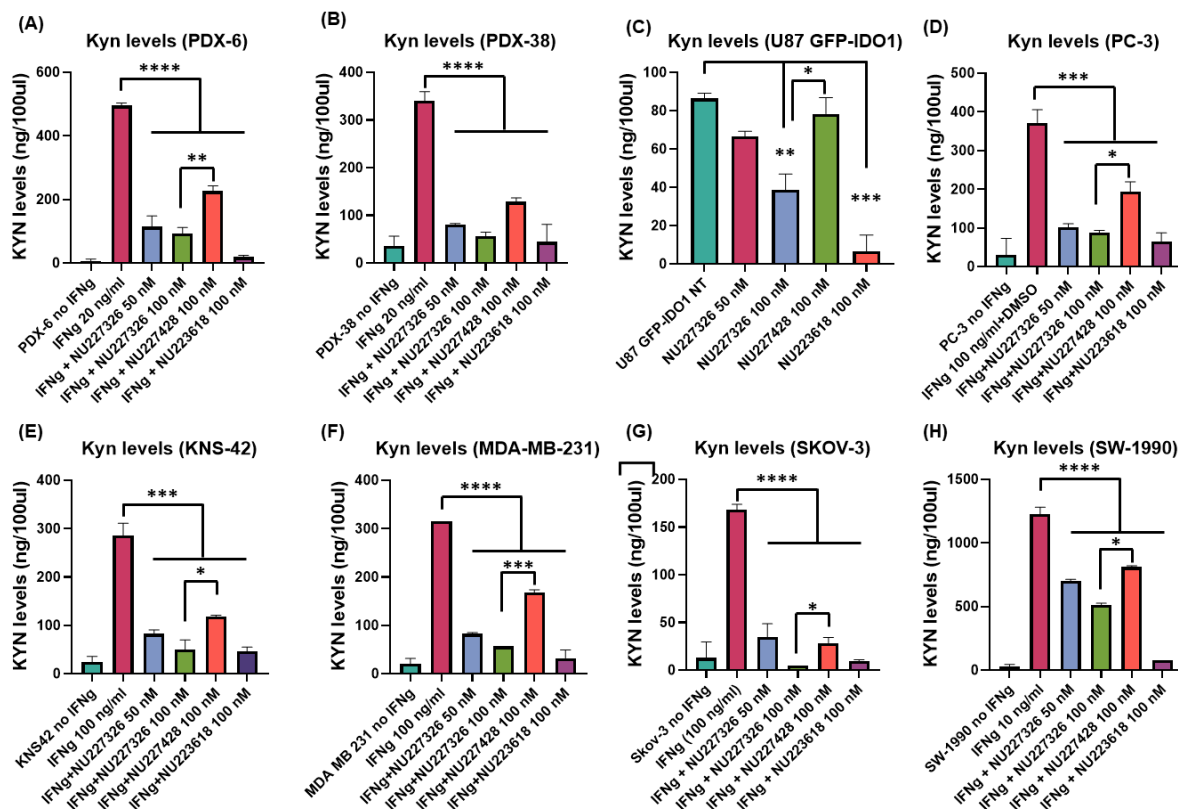


Figure S2. Inhibition of IDO1 enzyme activity by 21 (NU227326) in human cancer cell lines. Supernatants from various human cancer cell lines, including adult GBM patient-derived xenograft cells PDX-6 (A) and PDX-38 (B), U87 cells overexpressing GFP-fused IDO1 (C), prostate cancer PC-3 cells (D), pediatric GBM KNS42 cells (E), triple-negative breast cancer MDA-MB-231 cells (F), pancreatic cancer SW-1990 cells (G), and ovarian cancer SKOV-3 cells (H), were collected after 24-hour treatment with either compound **21** (NU227326), inactive PROTAC **24** (NU227428), or parental compound **4** (NU223618) at indicated concentrations. Kynurenine levels in the supernatants were measured using a modified Ehrlich method. Where indicated, cells were also treated with IFN γ at specified concentrations. Data are presented as mean \pm SEM. Statistical significance was determined using Tukey's multiple comparison test for comparisons between more than two groups and an unpaired Student's t-test for comparisons between two groups. Significance levels are indicated as follows: $P < 0.05$ (*), $P < 0.01$ (**), $P < 0.001$ (***), and $P < 0.0001$ (****).

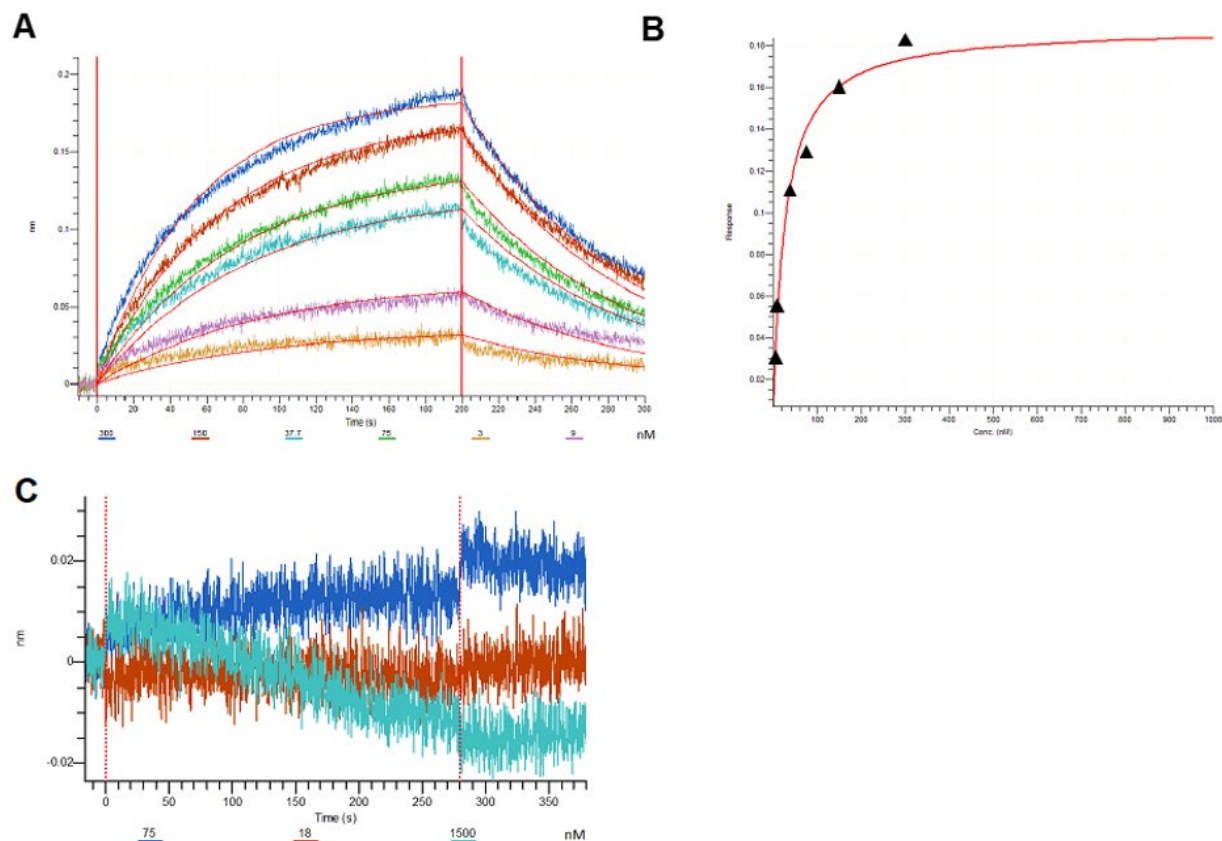
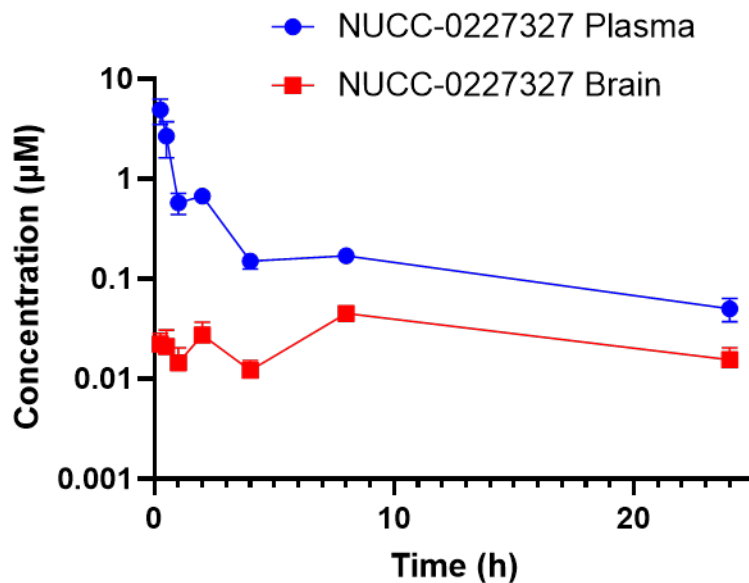


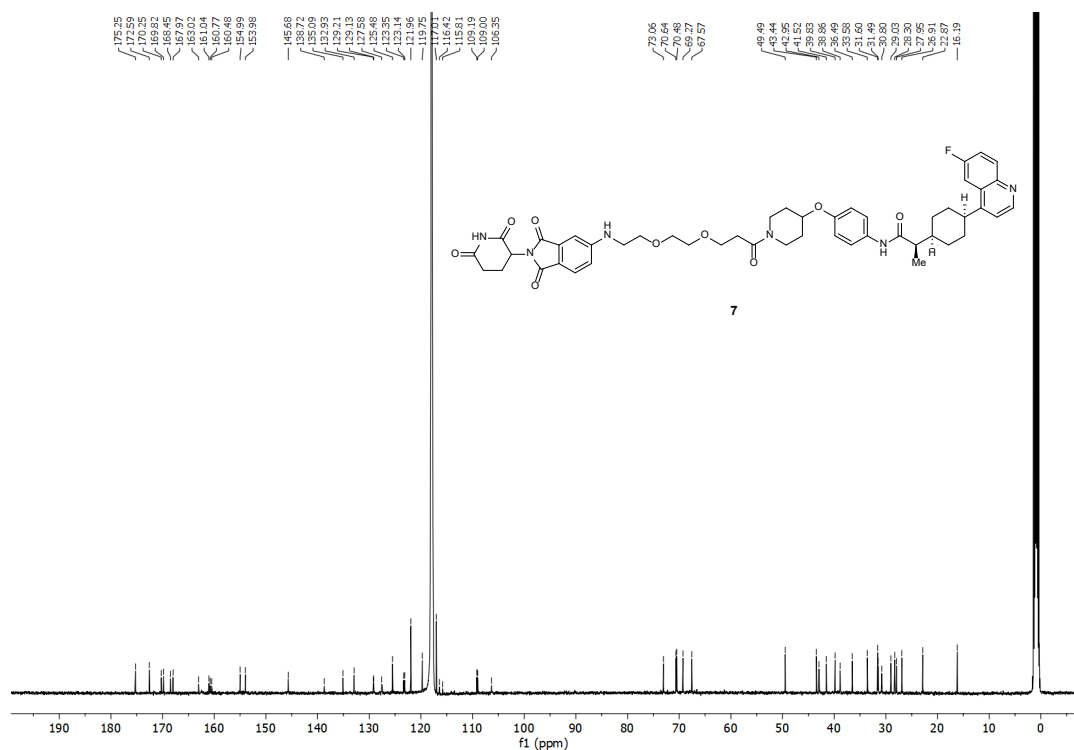
Figure S3. BLI data for Inactive IDO1 PROTAC **24** (NU227428). (A) BLI sensorgrams showing association and dissociation of compound **24** (NU227428) to IDO1 protein (loaded on NI NTA sensors). (B) The equilibrium dissociation constant (K_d) was obtained by fitting the steady state data (Req as a function of compound concentration) with a 1:1 binding model. The measured affinity (standard deviation) for the binary complex formed by IDO1 with **24** (NU227428) was determined to be 260 nM. (C) BLI sensorgrams monitoring the interaction of compound **24** (NU227428) with CRBN. CRBN was immobilized on AR2G sensors; the sensors were equilibrated in reaction buffer and then dipped into solutions of **24** (NU227428) (at concentrations indicated in the legend). No association between CRBN and **24** (NU227428) could be detected in these experiments.



Compound	Dose (mg/kg)	T _{1/2} (h)	T _{max} (h)	C _{max} (μM)	AUC _{0-∞} (μM·h)	AUC _{0-t} (μM·h)	MRT _{INF} (h)	Vz/F _{Obs} (mg/kg)/(μM)	CL/F _{obs} (mg/kg)/(μM)/h
NUCC-0227327 (plasma)	50	11.4	0.25	4.9	7.1	6.2	8.8	116.5	7.1
NUCC-0227327 (brain)	50	-	8.0	0.045	-	0.68	-	-	-

Figure S4. Pharmacokinetics of NU227327 (**20**). Several parameters could not be calculated for the brain samples because three points were not detected in the terminal elimination phase.

¹H-NMR and ¹³C-NMR Spectra of PROTAC 7



Chemical structure of compound **8** is shown above the spectrum. The structure features a phthalimide core linked via an ether and ester to a 4-chlorophenyl group, which is further connected to a 2-methyl-2-(quinolin-2-yl)ethyl group.

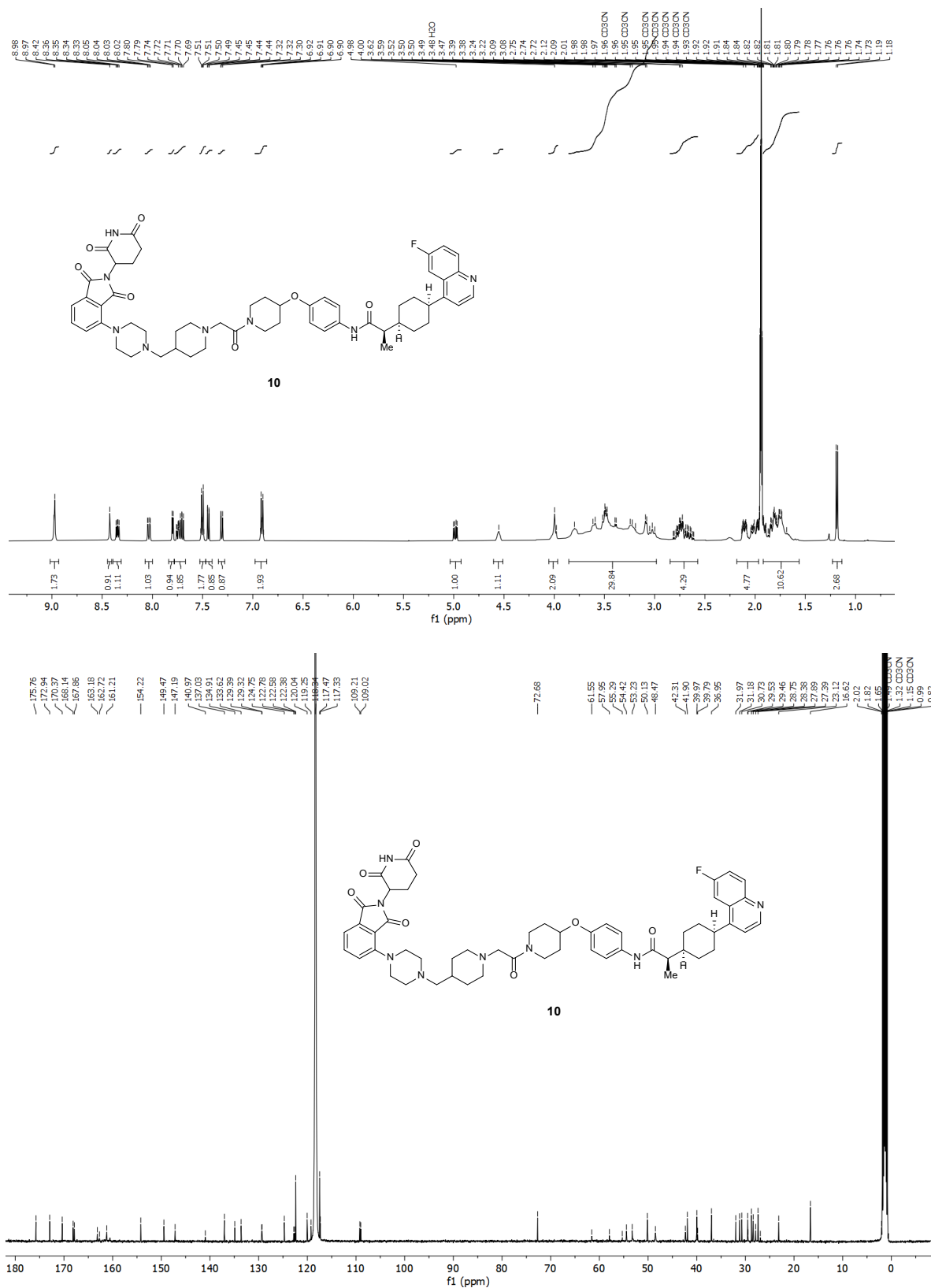
¹H NMR spectrum (CDCl₃) of compound **8**. The x-axis represents the chemical shift in ppm (f1), ranging from 1.15 to 9.95. The spectrum shows several multiplets in the aromatic region (6.5-8.5 ppm) and aliphatic region (1.1-2.1 ppm). Integration values are provided below the baseline for each major peak group.

Chemical Shift Range (ppm)	Integration Value
8.9 - 9.0	0.77
8.5 - 8.6	1.07
8.2 - 8.3	0.86
7.9 - 8.0	1.00
7.7 - 7.8	1.00
7.5 - 7.6	0.86
7.3 - 7.4	1.06
7.1 - 7.2	1.02
6.9 - 7.0	0.96
6.7 - 6.8	0.94
6.5 - 6.6	1.94
4.9 - 5.0	1.30
4.5 - 4.6	1.15
3.3 - 3.6	15.46
2.5 - 2.6	4.12
2.3 - 2.4	1.89
1.9 - 2.1	2.95
1.7 - 1.8	11.70
1.2 - 1.3	3.32

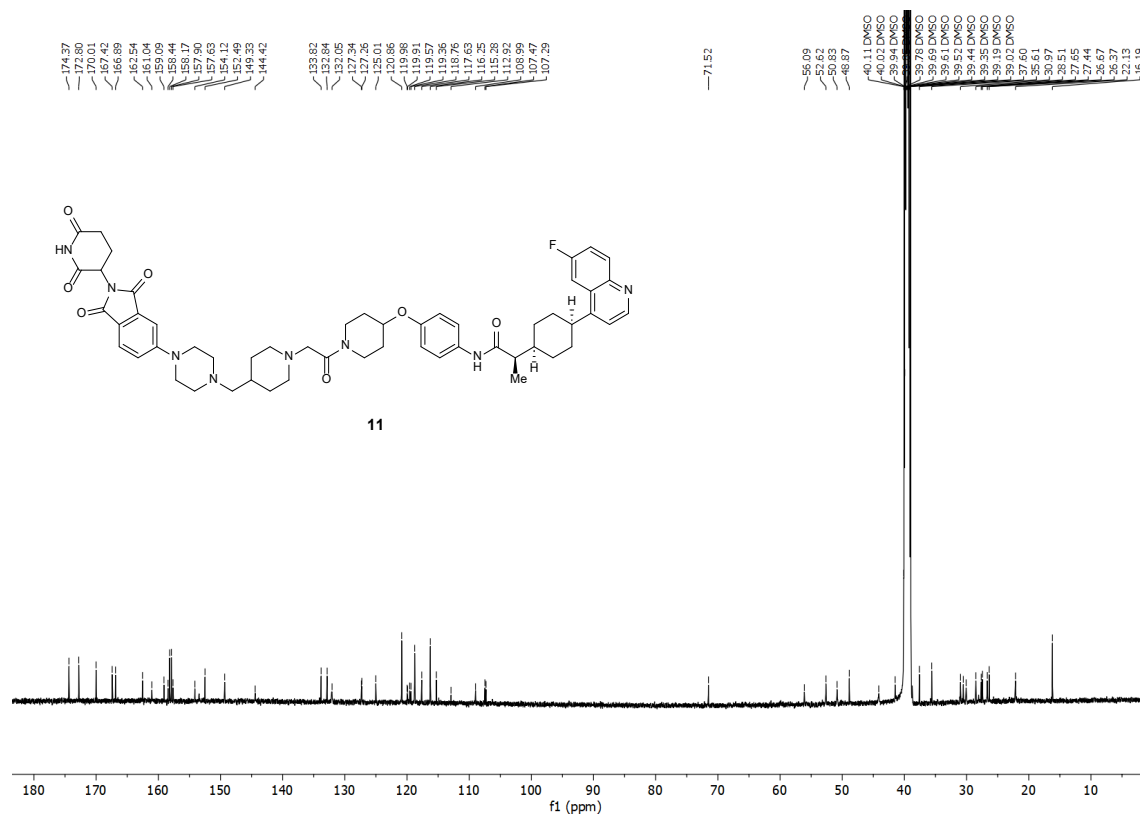
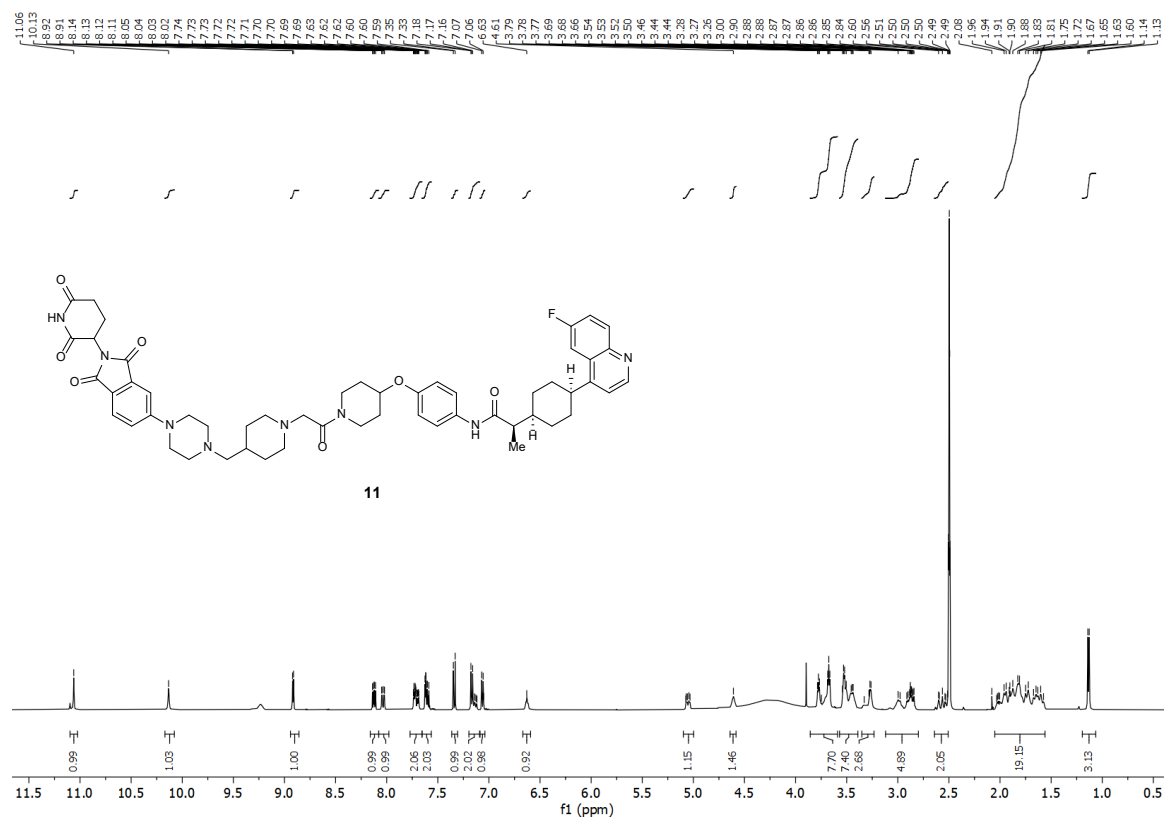


[illegible]

¹H-NMR and ¹³C-NMR Spectra of PROTAC 10



¹H-NMR and ¹³C-NMR Spectra of PROTAC 11

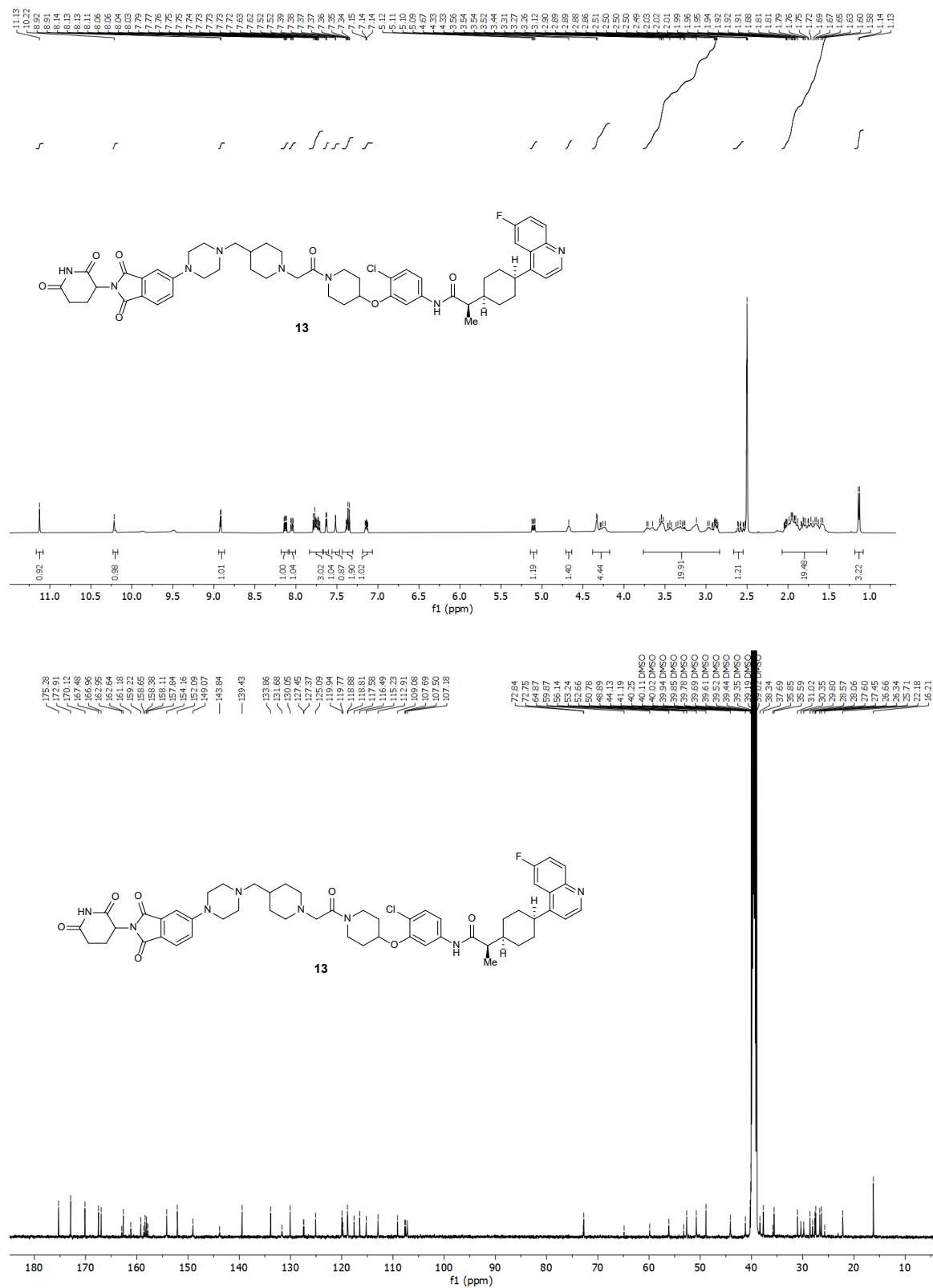


Chemical structure **12** is shown, which is a complex molecule featuring a benzimidazole core, a piperazine ring, a morpholine ring, a chlorophenyl group, a quinoline ring, and a fluorophenyl group. The structure is labeled **12**.

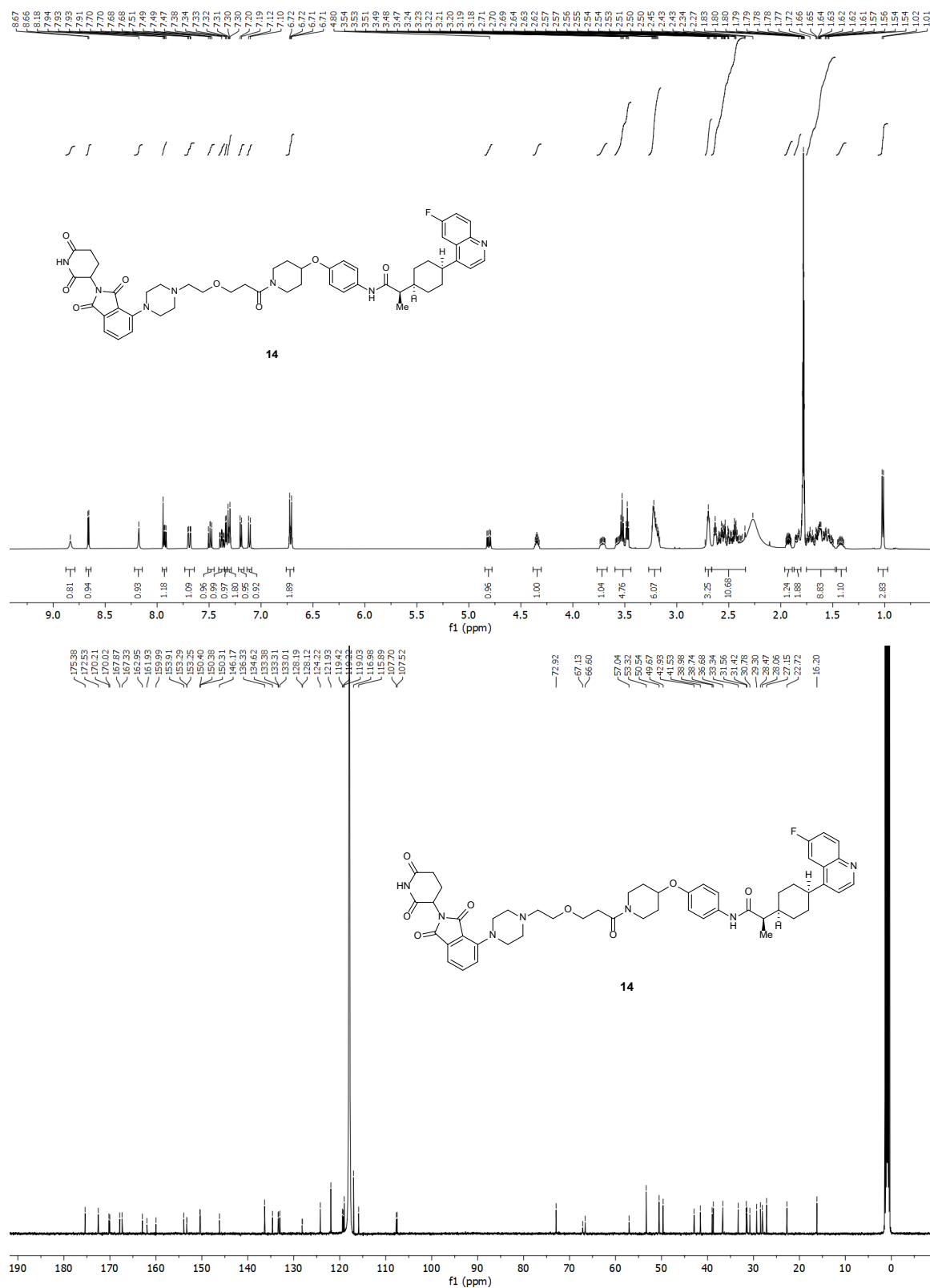
The ¹H NMR spectrum (top) shows peaks in the aromatic region (7.0-8.5 ppm) and aliphatic region (1.0-5.5 ppm). The x-axis is labeled f1 (ppm) and ranges from 0.5 to 10.0. Integration values are provided below the peaks.

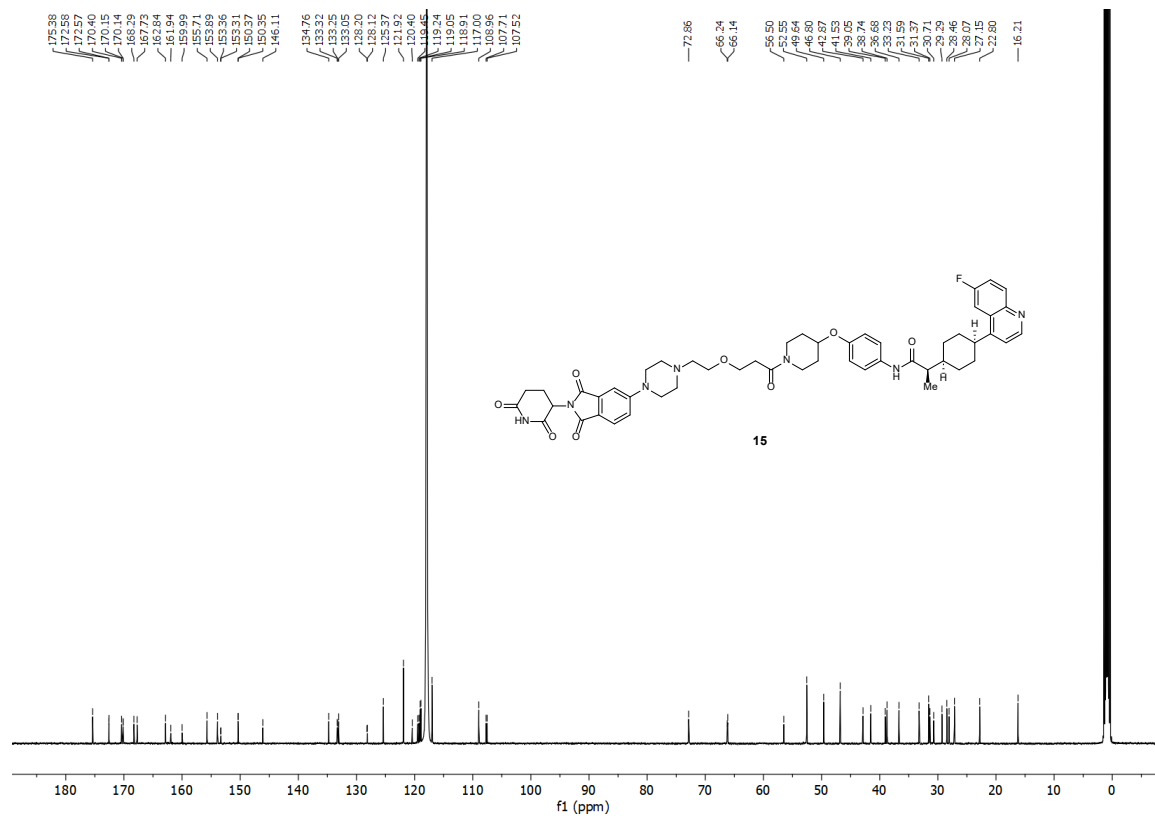
The ¹³C NMR spectrum (bottom) shows peaks in the aromatic region (100-180 ppm) and aliphatic region (15-75 ppm). The x-axis is labeled f1 (ppm) and ranges from -10 to 210. Integration values are provided below the peaks.

¹H-NMR and ¹³C-NMR Spectra of PROTAC 13

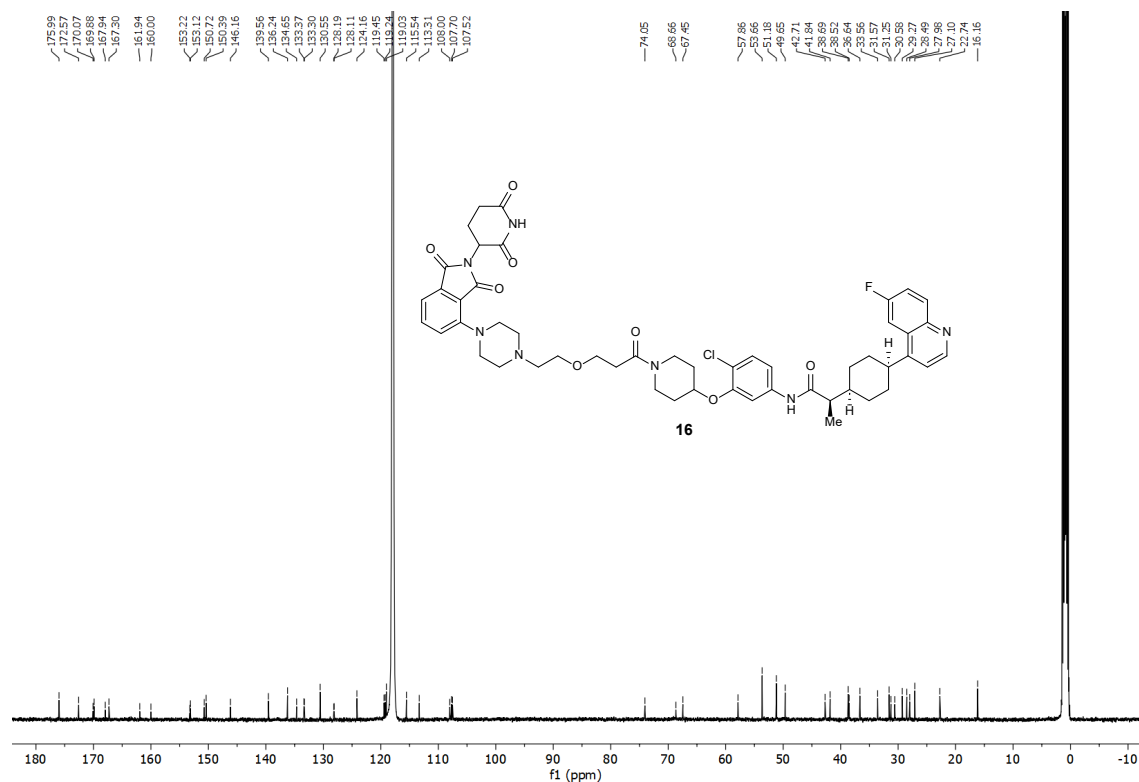
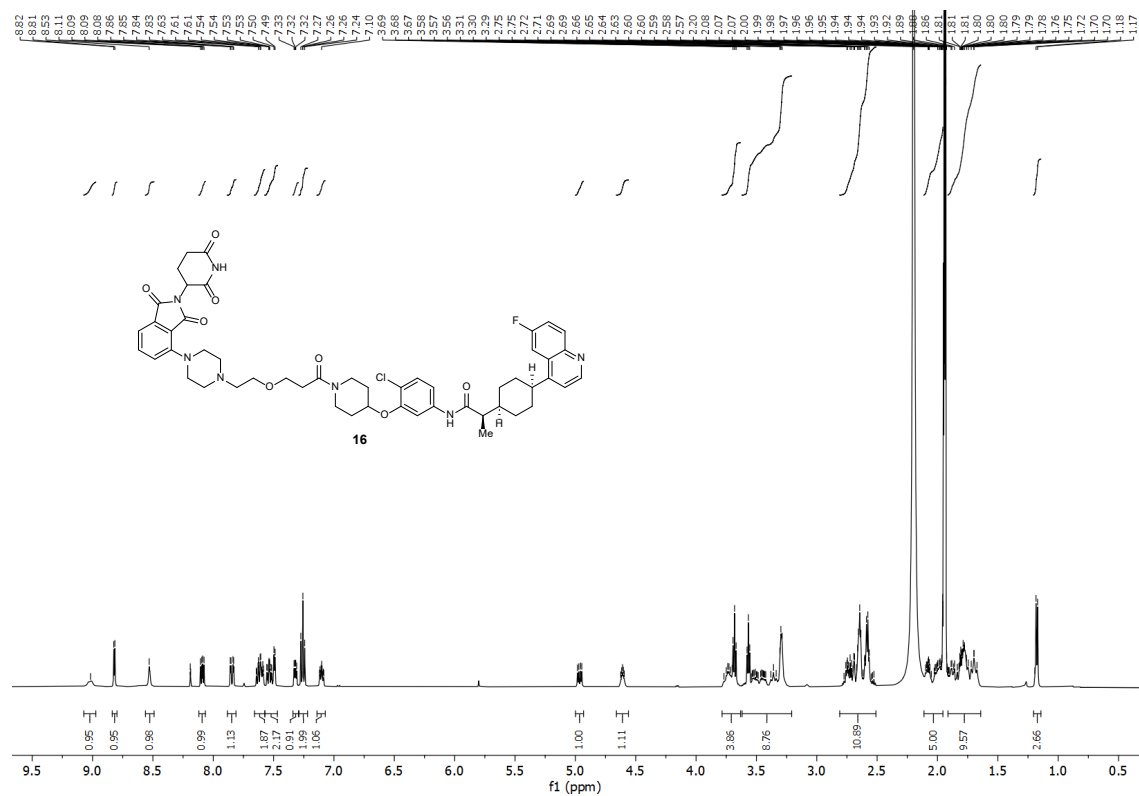


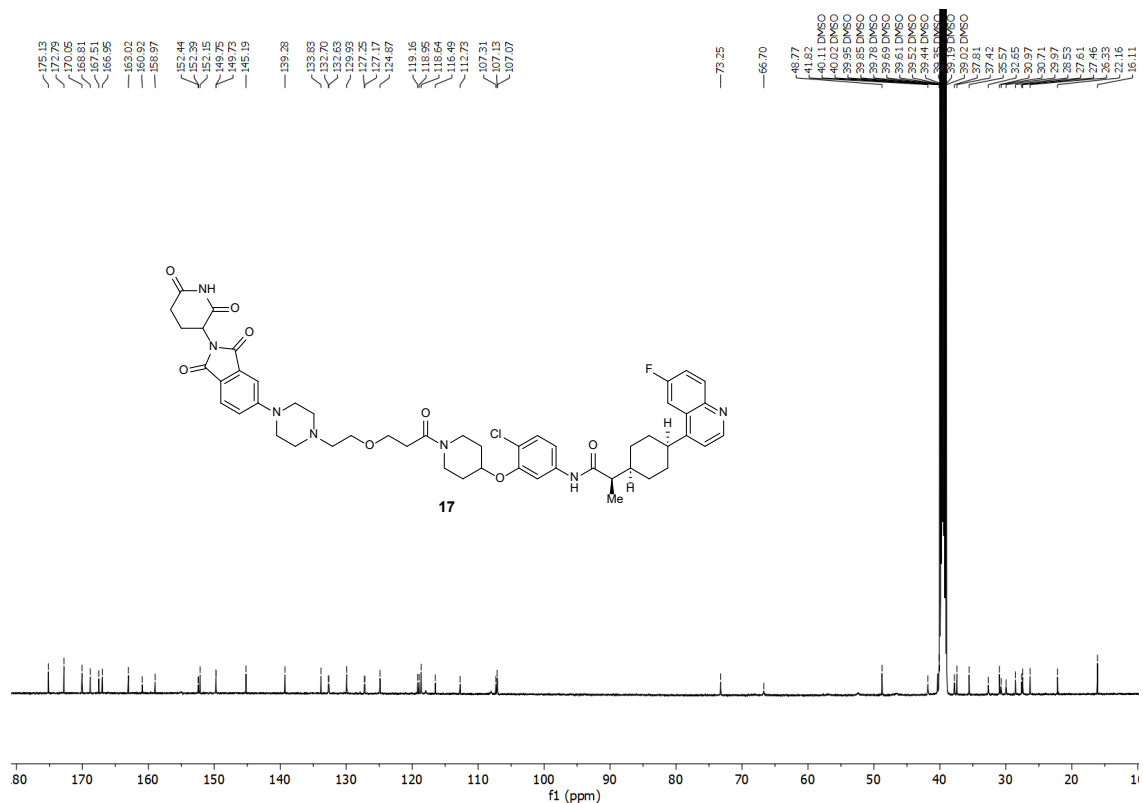
¹H-NMR and ¹³C-NMR Spectra of PROTAC 14



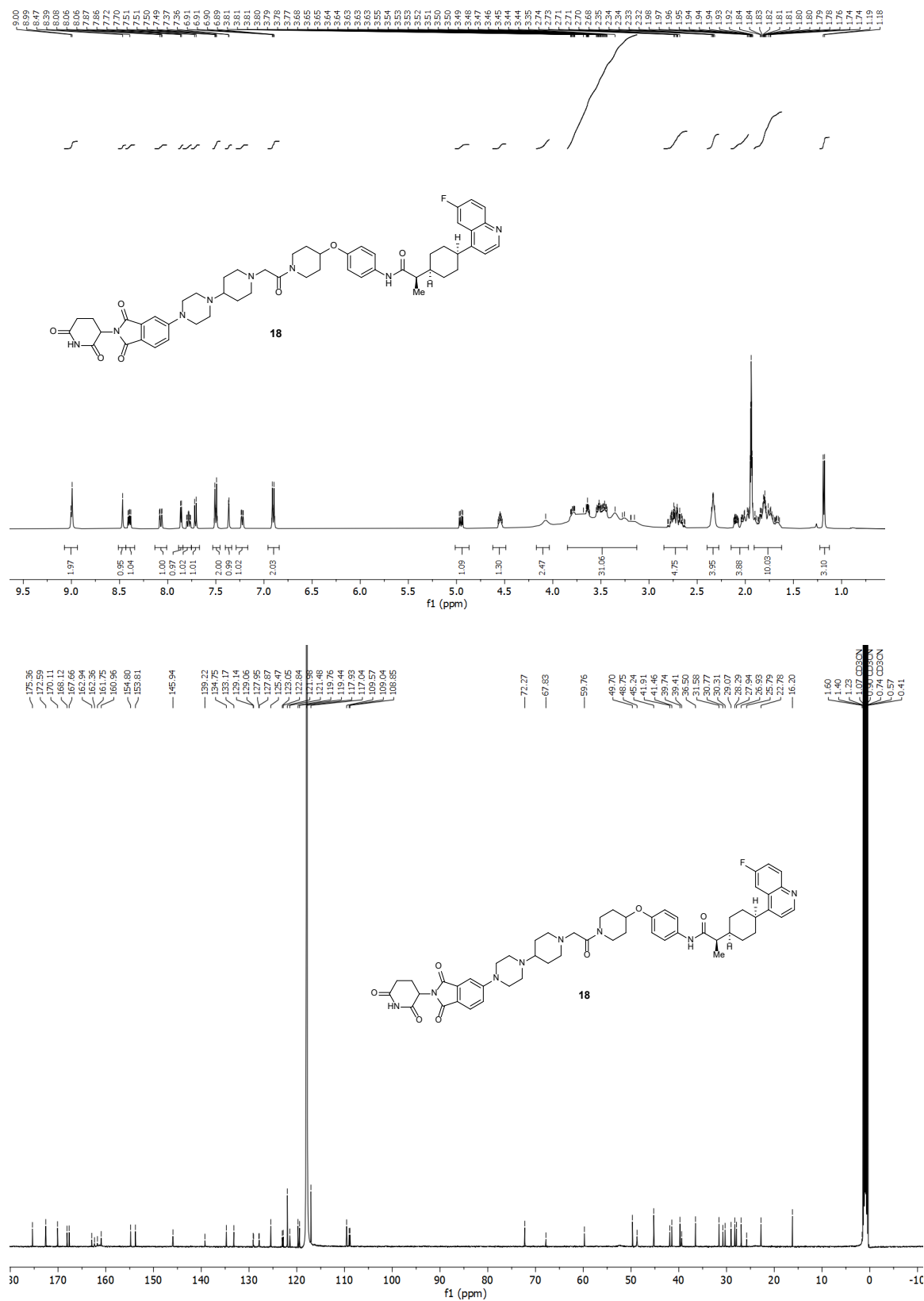


¹H-NMR and ¹³C-NMR Spectra of PROTAC 16

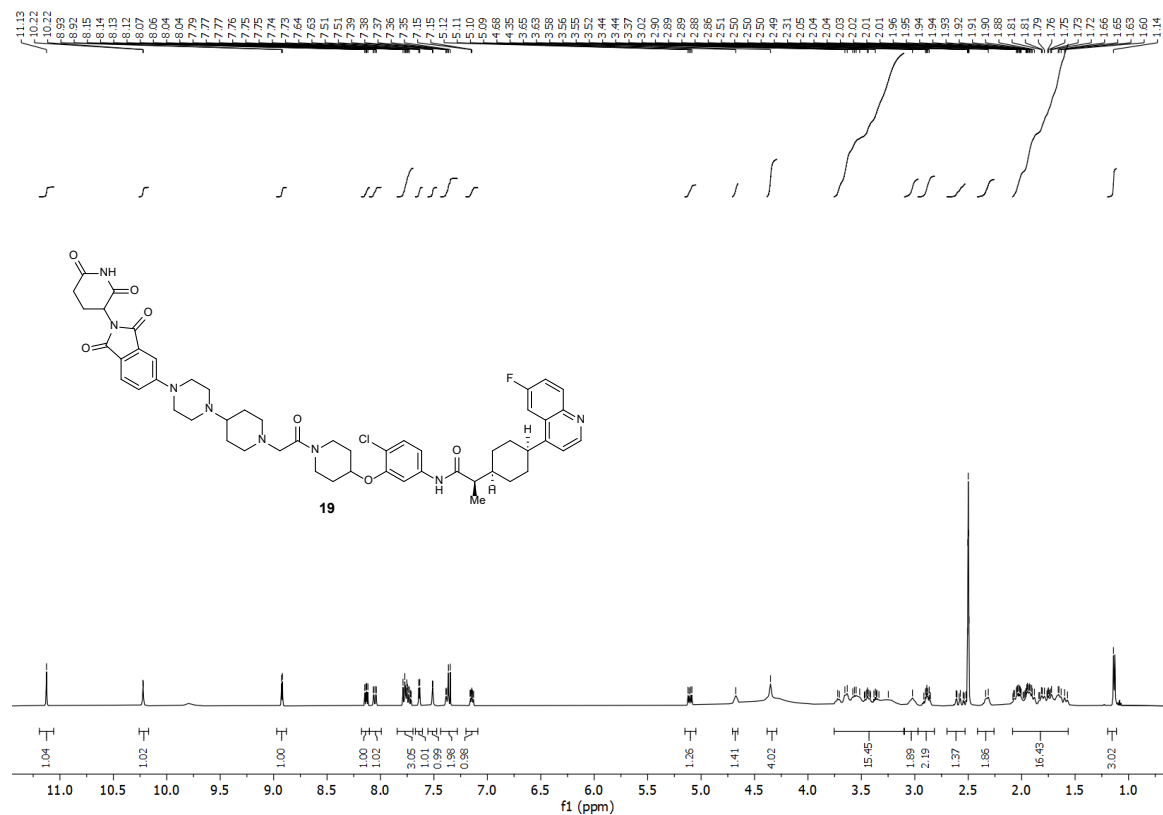




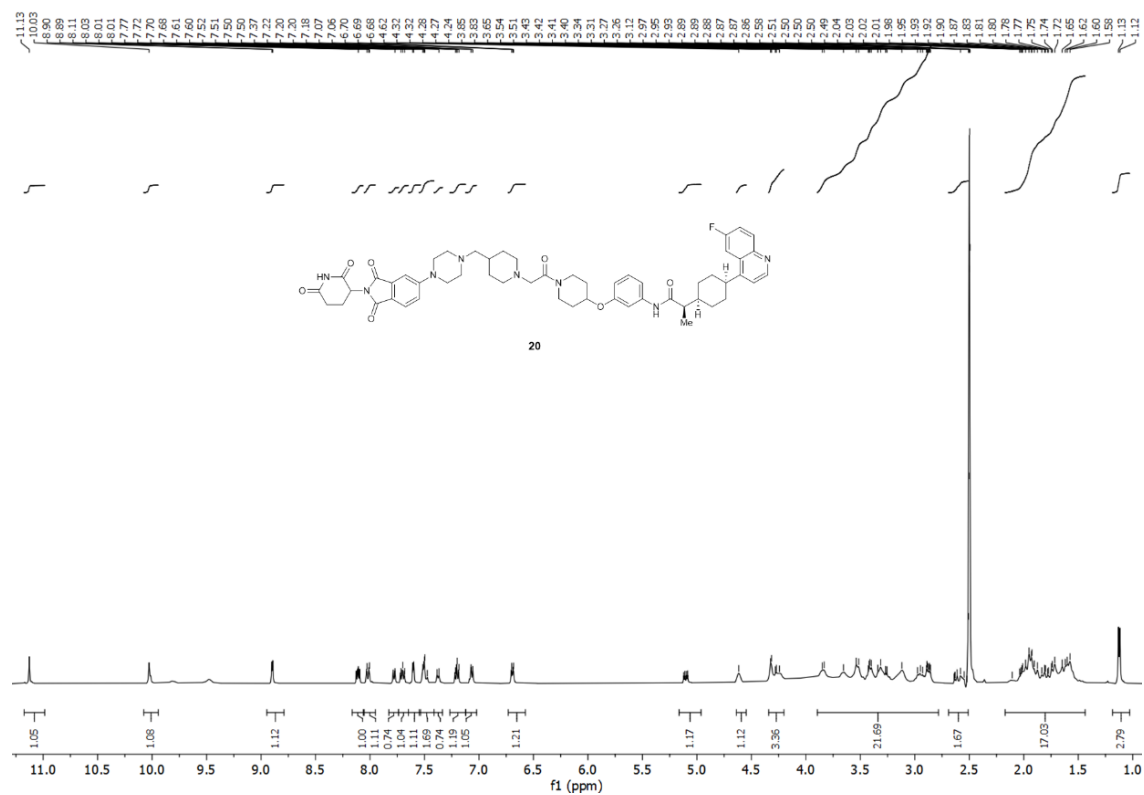
¹H-NMR and ¹³C-NMR Spectra of PROTAC 18



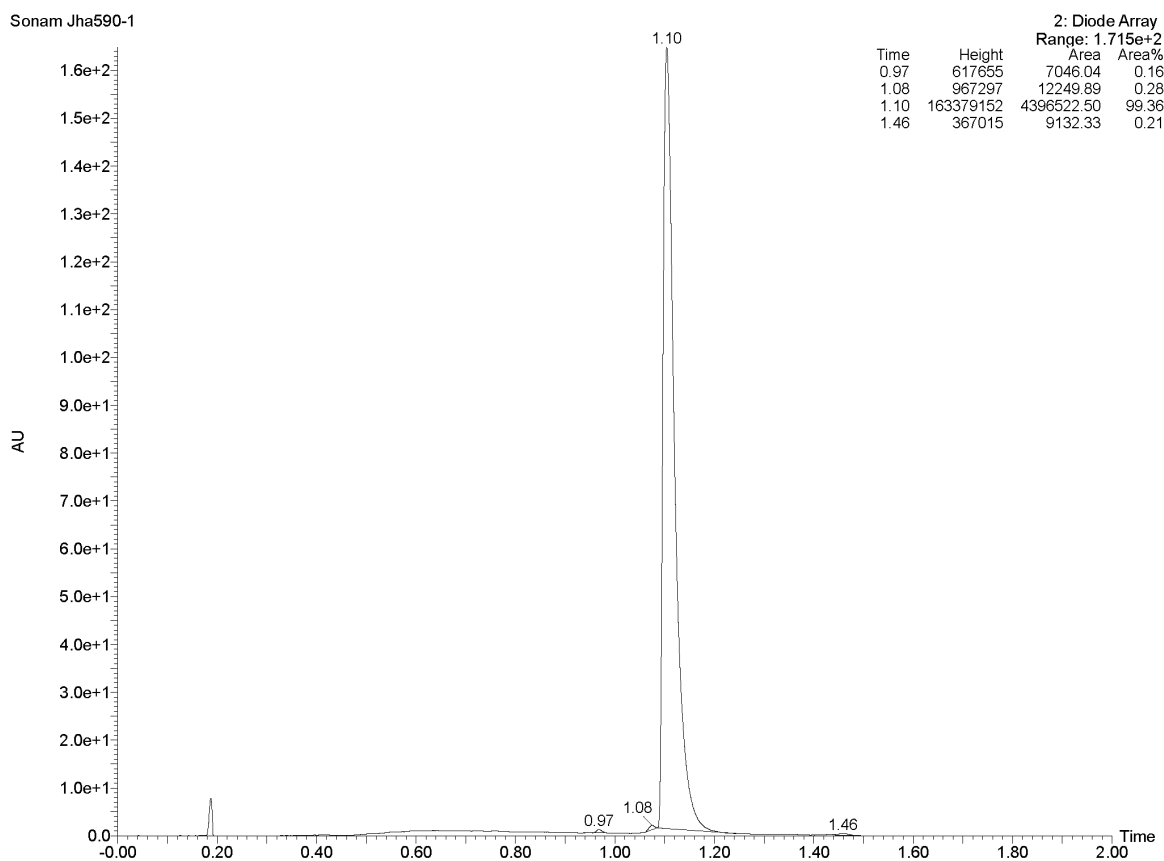
¹H-NMR and ¹³C-NMR Spectra of PROTAC 19



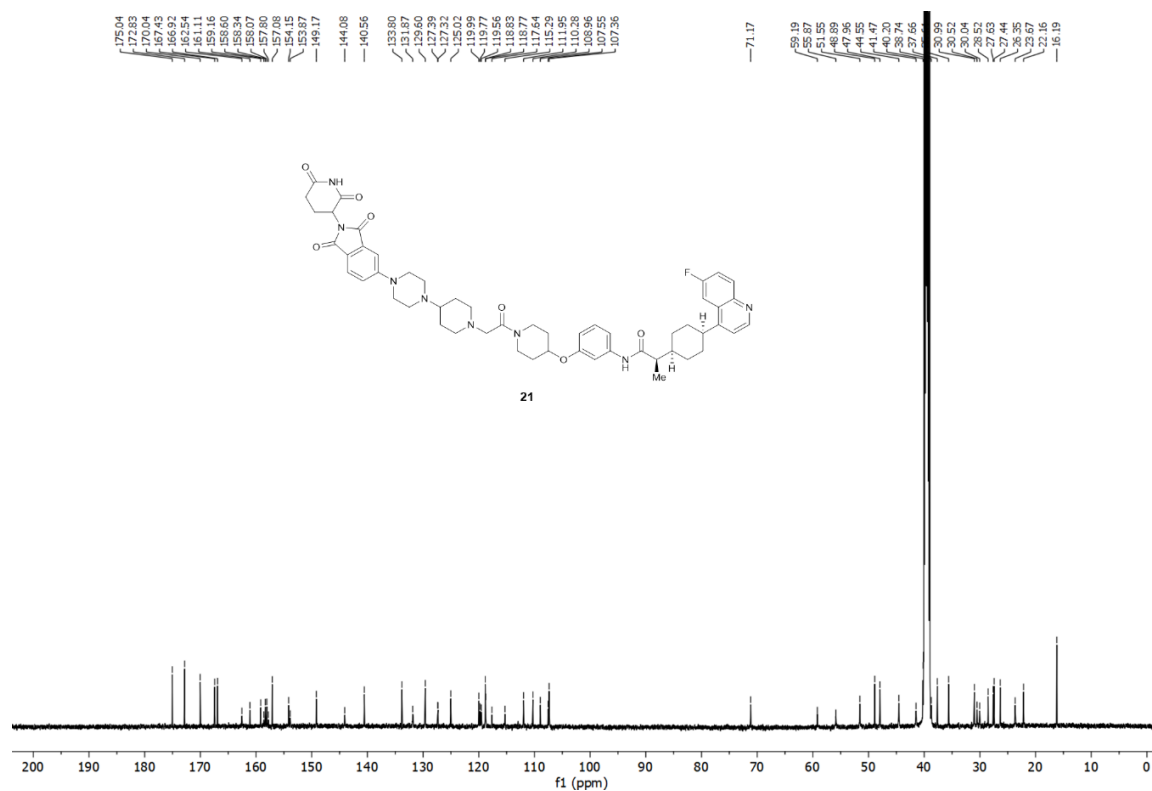
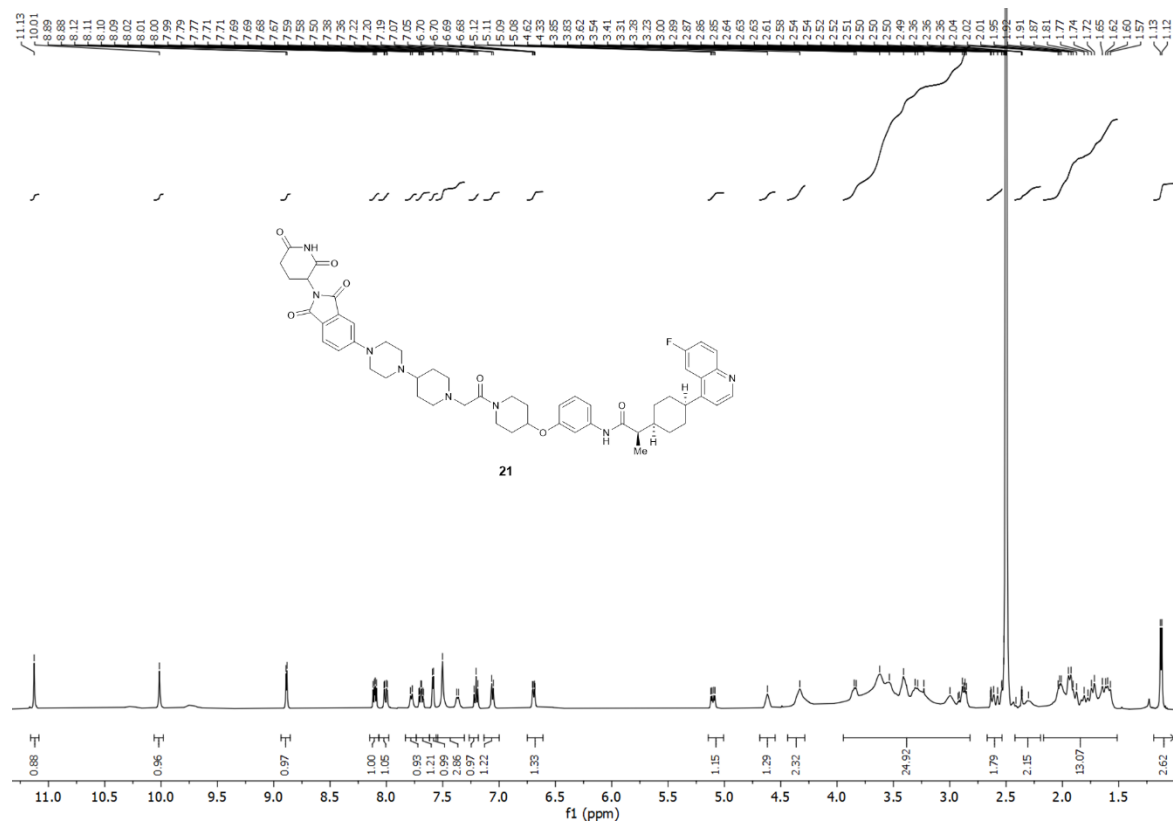
¹H-NMR and ¹³C-NMR Spectra of PROTAC 20



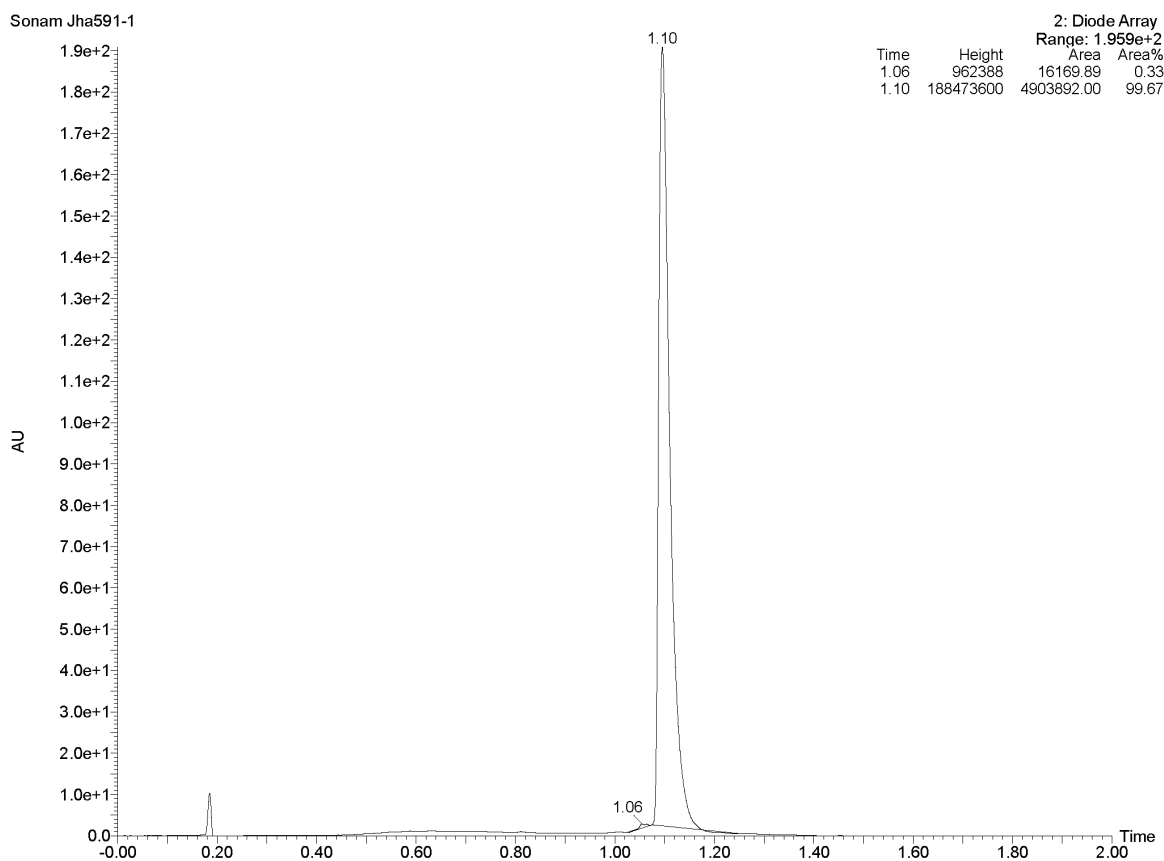
HPLC of Compound 20 (NU227326)



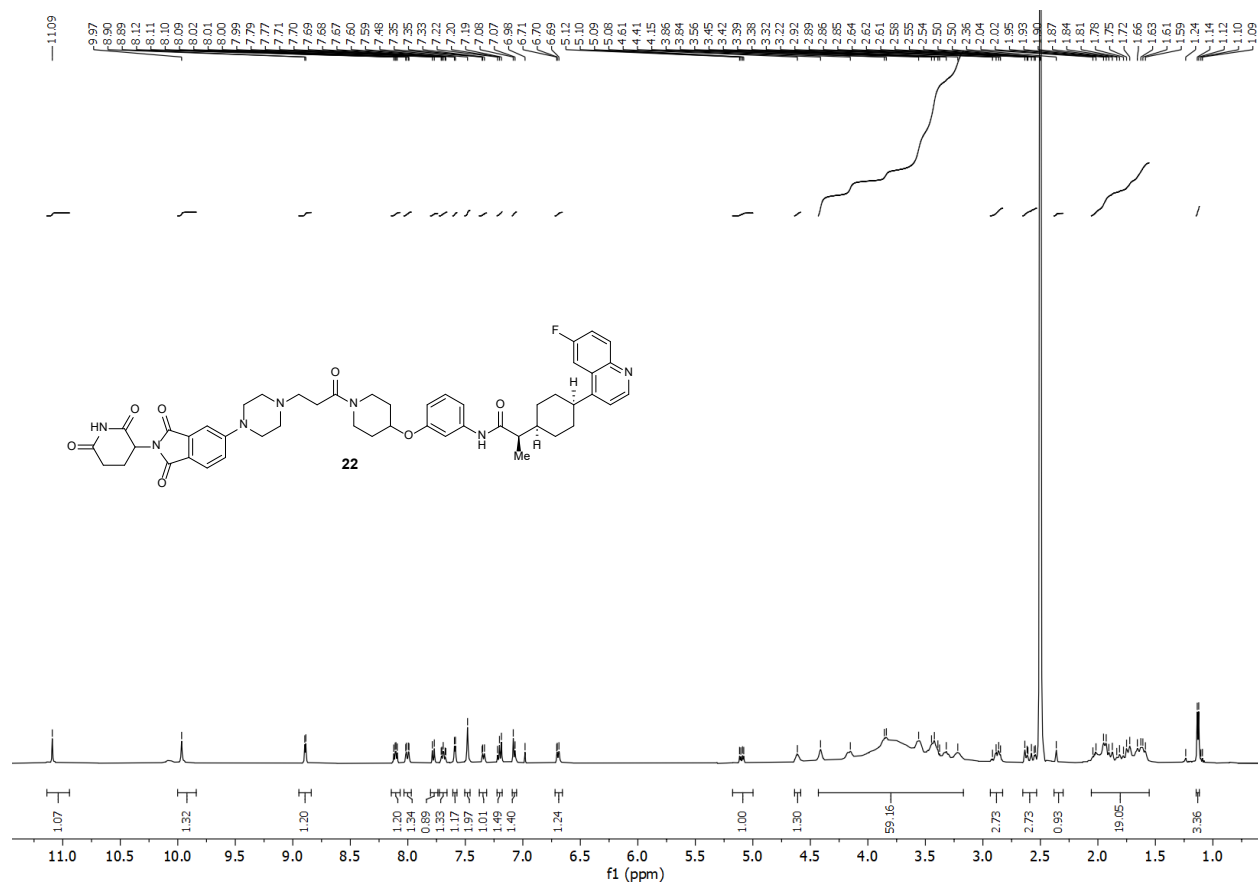
¹H-NMR and ¹³C-NMR Spectra of PROTAC 21



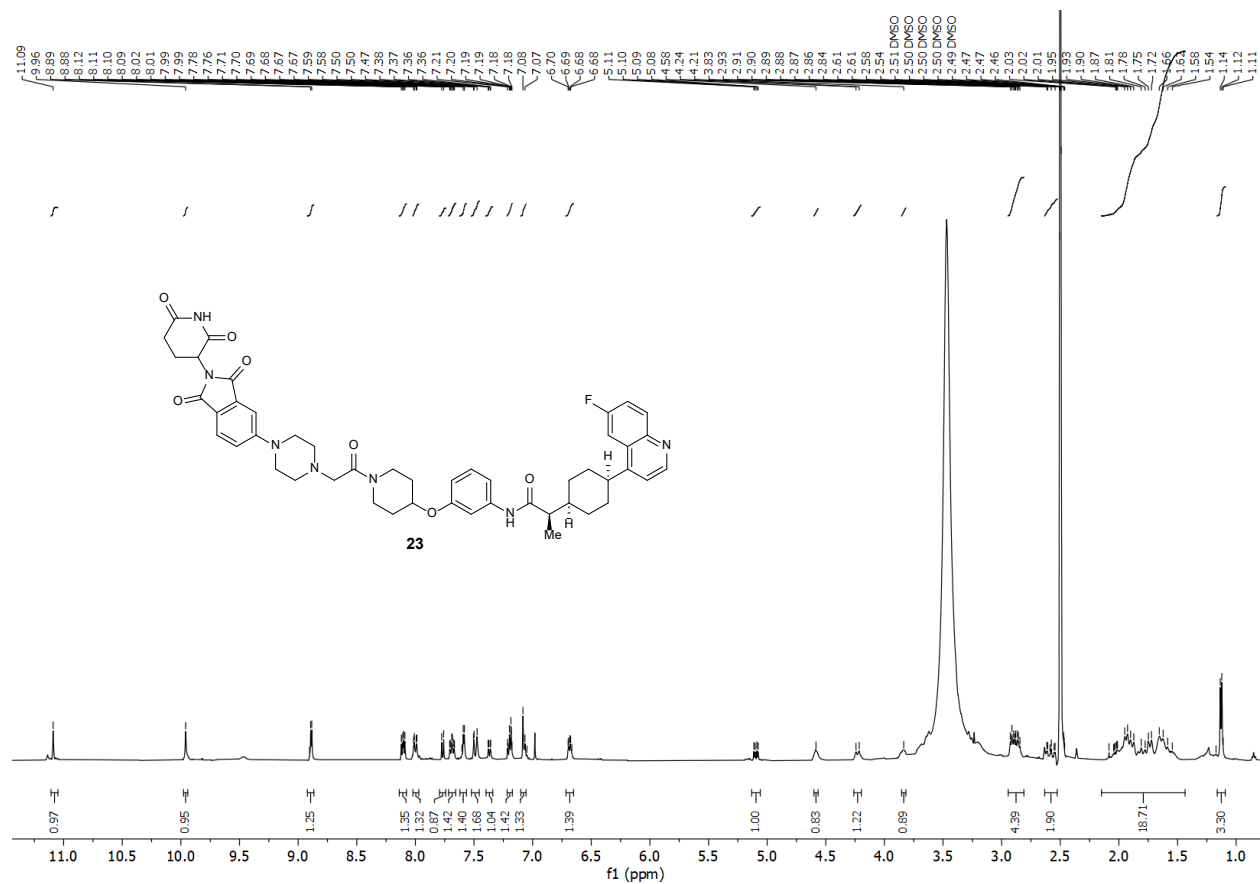
HPLC of Compound 21 (NU227327)



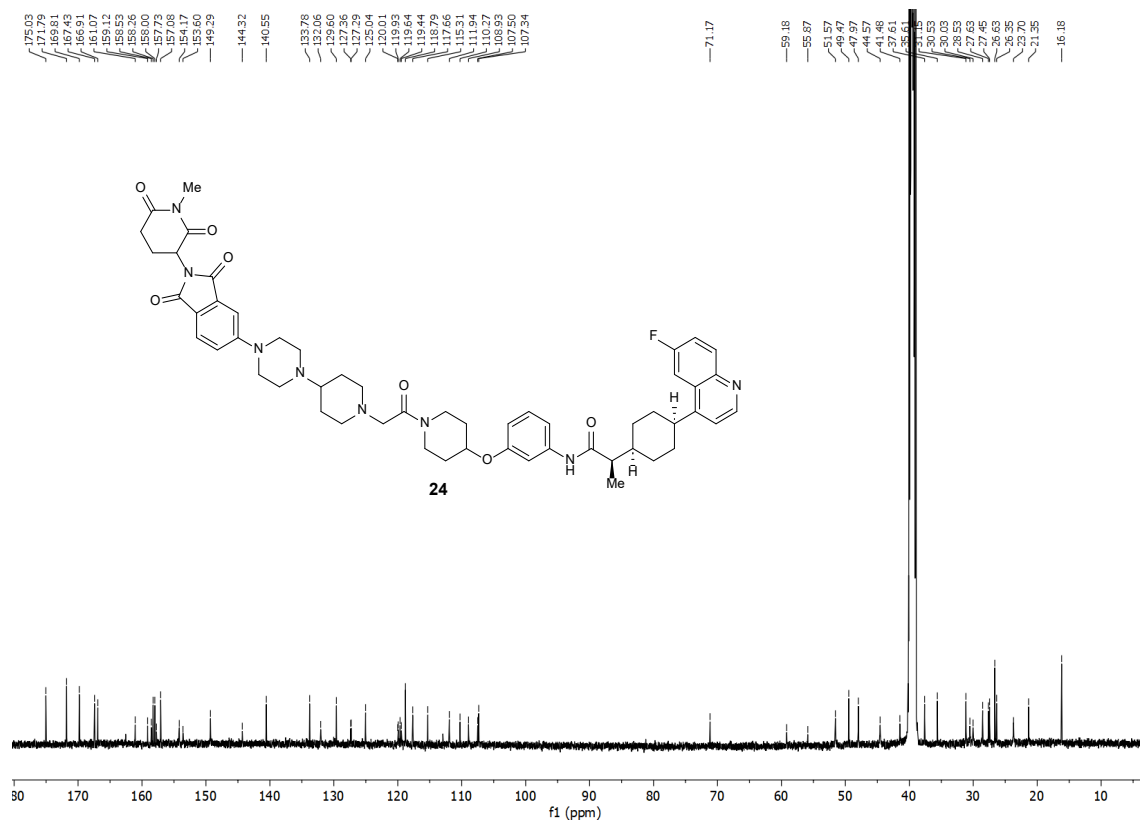
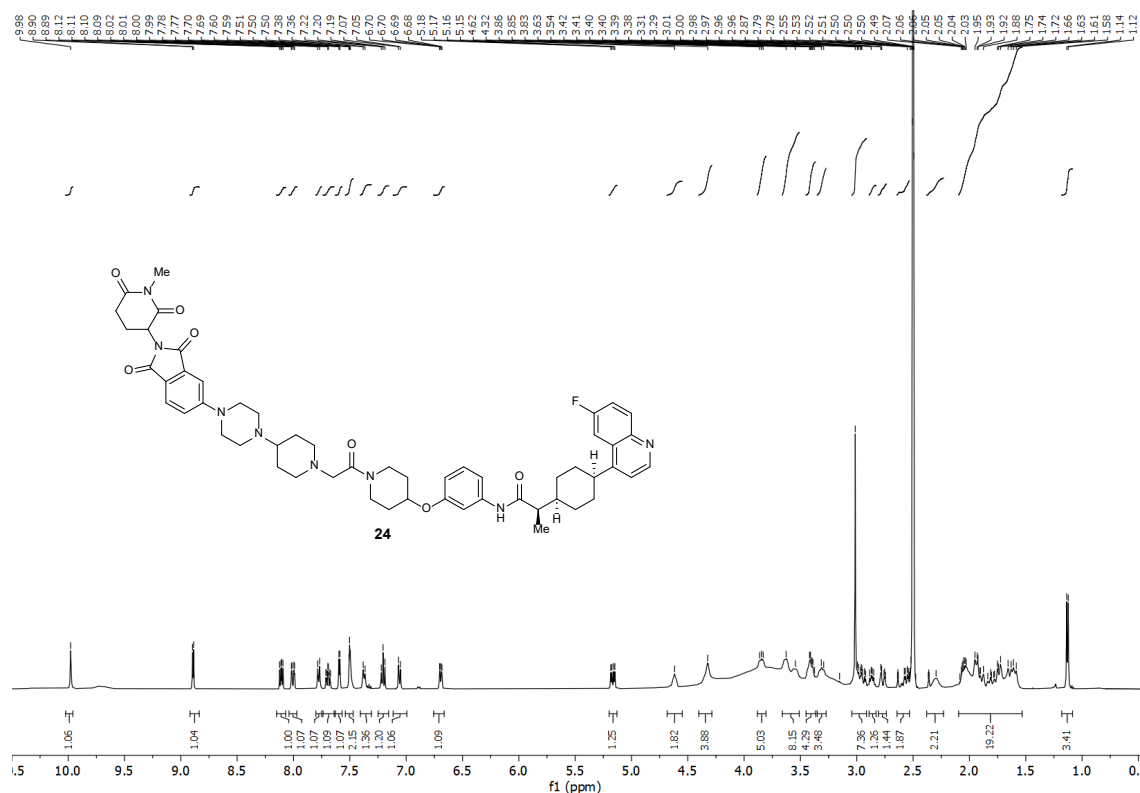
¹H-NMR Spectra of PROTAC 22



¹H-NMR Spectra of PROTAC 23



¹H-NMR and ¹³C-NMR Spectra of PROTAC 24



Raw data of Western Blot:

Below figures represents the expression of IDO1 and GAPDH obtained by Western Blot in Figure 5.

Figure 5: B

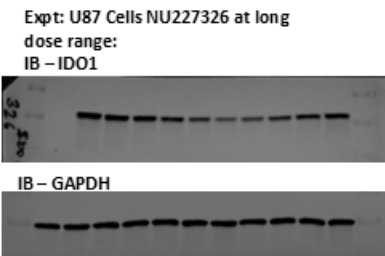


Figure 5: B

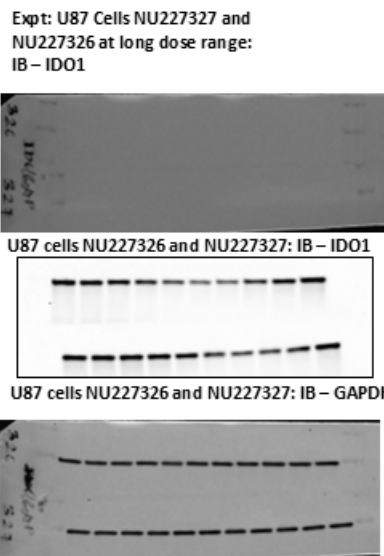


Figure 5: D

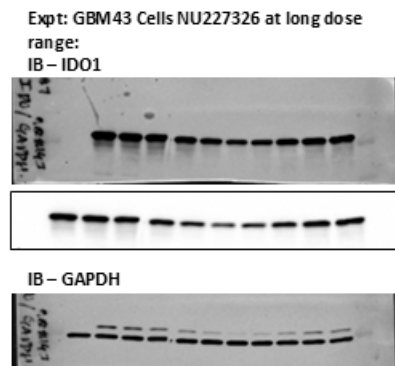


Figure 5: G

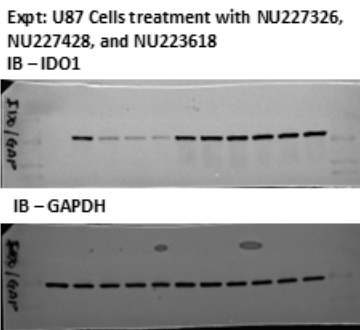


Figure S5. Raw western blot images used in Figure 5.

Below figures represents the expression of IDO1 and GAPDH obtained by Western Blot in Figure 6.

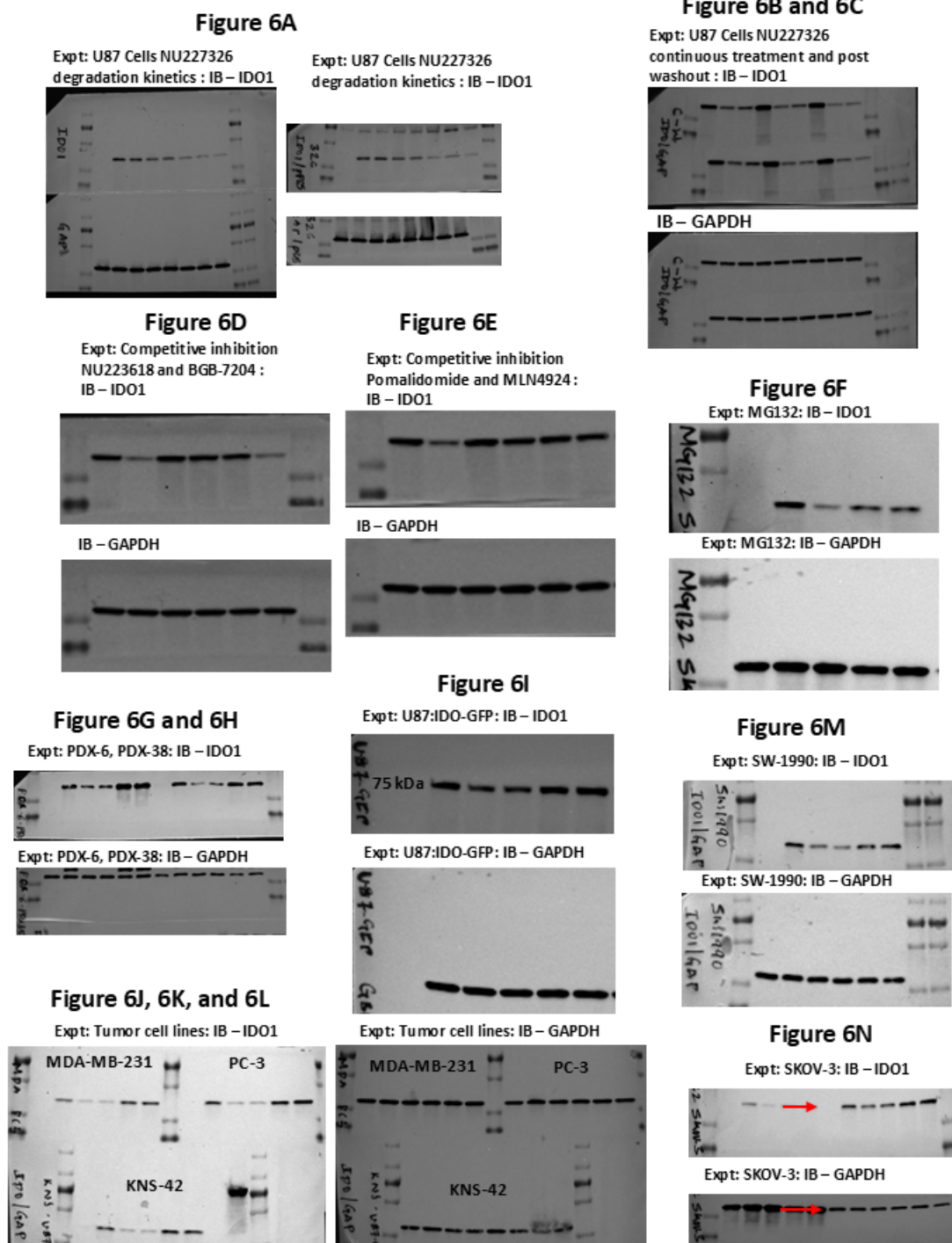


Figure S6. Raw western blot images used in Figure 6.